Electrochemical advanced oxidation of carbofuran in aqueous sulfate and/or chloride media using a flow cell with a RuO_2-based anode and an air-diffusion cathode at pre-pilot scale

Abdoulaye Thiam[a], Ricardo Salazar[b], Enric Brillas[c,]**, Ignasi Sirés[c,]*

[a] *Programa Institucional de Fomento a la I+D+i, Universidad Tecnológica Metropolitana, Ignacio Valdivieso 2409, Santiago, Chile.*

[b] *Laboratorio de Electroquímica Medioambiental, Universidad de Santiago de Chile, Av. Libertador Bernardo O'Higgins 3363, Santiago, Chile.*

[c] *Laboratori d'Electroquímica dels Materials i del Medi Ambient, Departament de Química Física, Universitat de Barcelona, Martí i Franquès 1-11, 08028 Barcelona, Spain.*

Paper submitted for publication in *Chemical Engineering Journal*

Corresponding author: * E-mail: i.sires@ub.edu (I. Sirés)

** E-mail: brillas@ub.edu (E. Brillas)

Abstract

The treatment of 0.348 mM carbofuran solutions in 0.050 M Na_2SO_4 at pH 3.0 has been studied by electrochemical oxidation with electrogenerated H_2O_2 (EO-H_2O_2), electro-Fenton (EF) and photoelectro-Fenton (PEF). The trials were performed in a 2.5 L pre-pilot plant equipped with a filter-press cell, which contained a RuO_2-based anode and an air-diffusion cathode, connected to an annular photoreactor with a 160 W UVA lamp in PEF. The oxidizing species were the $^{\bullet}OH$ generated at the anode from water oxidation and in the bulk from Fenton's reaction between added Fe^{2+} and H_2O_2 produced at the cathode. The oxidation power of treatments rose in the order EO-H_2O_2 << EF < PEF, demonstrating the preponderant role of $^{\bullet}OH$ in the bulk. The drug decay always obeyed a pseudo-first order kinetics. Similar TOC abatements of 82%-88% were found in PEF operating at different current densities and carbofuran concentrations, ascribed to the additional photolytic action of UVA light to remove photoactive intermediates, also allowing a gradual detoxification. In matrices with Cl^-, active chlorine was also produced as oxidant and its quick reaction with carbofuran caused its faster decay at increasing Cl^- content. However, lower mineralization was achieved because of the accumulation of recalcitrant chloroderivatives. GC-MS analysis of treated solutions with 0.070 M NaCl corroborated the formation of 6 chloroderivatives, whereas 5 heteroaromatics were detected in 0.050 M Na_2SO_4. Oxalic acid was accumulated in the latter medium since its Fe(III) complexes were stable in EF and rapidly mineralized by UVA light in PEF. The mineralization of urban wastewater spiked with carbofuran by PEF in the pre-pilot plant was partial due to the recalcitrant chloroderivatives formed from carbofuran and natural organic matter.

Keywords: Carbofuran; Electrochemical oxidation; Electro-Fenton; Photoelectro-Fenton; Wastewater treatment

1. Introduction

Remediation of wastewater contaminated with agricultural pesticides has been recognized as a major environmental concern because of the ineffectiveness of traditional physicochemical and biological methods used in municipal wastewater treatments plants (WWTPs) [1-3]. Removal of these residues, which eventually affect food and drinking water, is necessary to avoid various diseases in human beings [3-5]. Carbofuran (2,3-dihydro-2,2-dimethylbenzofuran-7-yl methylcarbamate, see physicochemical characteristics in Table S1) is a well-known methylcarbamate pesticide, widely used to inhibit insect activity in soybean, rice, sugar cane, tobacco, maize, potatoes and vegetables. It accounts for about 12.4% of the annual production of insecticide in developing countries [6]. The use of carbofuran is worrisome not only due to its massive use but also because of its high oral toxicity [7]. It has been detected in soil as well as in wastewater, natural water and drinking water owing to its high solubility and mobility, with a half-life of 30-117 days [8-11]. The United States Environmental Protection Agency recommends a maximum acceptable carbofuran concentration in potable drinking water of 0.09 mg L^{-1}, whereas a lower value of 3 µg L^{-1} is admitted by the World Health Organization [12]. This insecticide can produce diabetes and cancer in humans and others diseases in animals and can act an inhibitor of acetyl cholinesterase, an enzyme vital to control nervous system, being an endocrine disruptor [13-16]. Due to its refractory character to conventional degradation treatments, effective and inexpensive methods are needed for removing this hazardous insecticide from water.

Over the past three decades, different advanced oxidation processes (AOPs) have been developed to treat wastewater contaminated with toxic and biorefractory organic compounds. They are chemical, electrochemical (EAOPs) and photo-assisted processes characterized by their ability to produce highly reactive hydroxyl radical ($^{\bullet}OH$) on site. This radical is able to oxidize most organics up to their mineralization to CO_2, water and inorganic ions, thanks to its high standard redox potential of $E^{o}(^{\bullet}OH/H_2O)$ = 2.80 V/SHE along with high rate constants (10^7-10^{10} $M^{-1}s^{-1}$) to

react with organic molecules [17-20]. Several authors have reported the effective treatment of aqueous carbofuran solutions by chemical and photochemical AOPs including O_3 and O_3/UV [21], ultrasound [22], chemical Fenton (H_2O_2/Fe^{2+} mixture) [22], UV/H_2O_2 [23] and photo-Fenton (UV/H_2O_2/Fe^{2+}) [24,25]. The use of EAOPs like pulsed corona discharge [26], low temperature plasma [27], anodic Fenton treatment [28], electrochemical oxidation (EO) with a boron-doped diamond anode (BDD) [29] and electro-Fenton (EF) with Pt/carbon-felt [25,30] and BDD/carbon-felt [29] cells has also been described. In EF with a BDD/carbon-felt cell, the most powerful EAOP tested so far, total insecticide disappearance and almost total mineralization were achieved after 60 and 360 min of electrolysis of 250 mL of 0.125 mM carbofuran in 0.050 M Na_2SO_4 at pH 3.0 and 300 mA [29]. In the above EO and EF processes, complete release of initial N as NH_4^+ ion was found [25,29,30]. However, none of the published studies on EAOPs has taken into account other important aspects to confirm their viability for carbofuran degradation, as for example the effect of different electrolytes, the organic intermediates formed along the degradation, the influence of UV radiation in processes like photoelectro-Fenton (PEF), the evaluation of current efficiencies and energy consumption and the time course of ecotoxicity. The treatment in pre-pilot plants has been disregarded as well, despite being a key step for the scale up of the electrochemical treatments.

This paper aims to clarify the degradation of carbofuran in aqueous matrices by EAOPs like EO with electrogenerated H_2O_2 (EO-H_2O_2), EF and, especially, PEF with UVA light, which has not been investigated so far. The trials were carried out in a 2.5 L pre-pilot plant equipped with a flow cell that included a RuO_2-based anode and a carbon-polytetrafluoroethylene (PTFE) air-diffusion cathode. Coupling with a 160 W UVA lamp centered in an annular glass photoreactor was needed in PEF. The anode was chosen because we have very recently demonstrated that IrO_2- and RuO_2-based dimensionally stable anodes can act as viable, low cost materials to degrade organic pollutants such as Ponceau 4R, naproxen and methylparaben by PEF [31-33]. They may yield similar mineralization current efficiencies, but with lower energy consumption, as compared to

more powerful but expensive anodes like BDD. Note that higher carbofuran concentrations (usually 0.348 mM) than those found in WWTPs were treated, aiming to clearly assess its decay kinetics and mineralization profiles upon application of the three EAOPs in all aqueous matrices under comparable conditions. The influence of current density (*j*), catalyst and insecticide concentrations on the performance of the PEF process was examined as well. The first part of the work was carried out in an inert electrolyte like Na_2SO_4 in order to assess the role of homogeneous and heterogeneous hydroxyl radicals, whereas in the second part different matrices containing chloride were employed to evaluate the benefits or drawbacks of active chlorine co-generation. Organic intermediates formed by PEF in both media were identified by gas chromatography-mass spectrometry (GC-MS) and final carboxylic acids were quantified by ion-exclusion high-performance liquid chromatography (HPLC). The change of ecotoxicity with time during the different EAOPs in sulfate medium was determined from the bioluminescence inhibition of the marine bacteria *Vibrio fischeri*. Finally, a PEF test was made by spiking the insecticide into real urban wastewater.

2. Materials and methods

2.1. Reagents

Carbofuran (98% purity) was purchased from Sigma-Aldrich and used as received. Anhydrous sodium sulfate and sodium chloride, used as background electrolytes, and iron(II) sulfate heptahydrate, used as catalyst, were of analytical grade supplied by Fluka, Merck and Sigma-Aldrich, respectively. The solutions were prepared with deionized water. Concentrated sulfuric and hydrochloric acids, used for pH adjustment to 3.0, were of analytical grade supplied by Panreac. The other chemicals were either of HPLC or analytical grade purchased from Merck and Panreac.

2.2. Urban wastewater

A single set of urban wastewater was collected downstream after the secondary treatment in a WWTP in Gavà (Barcelona, Spain) in October 2016. It was preserved in a refrigerator at 4 ºC

before use and presented the following characteristics: pH 7.9, specific conductivity of 3.2 mS cm^{-1}, 15.0 mg L^{-1} of total organic carbon (TOC), 0.19 mg L^{-1} Fe^{2+}, 36.9 mg L^{-1} NH_4^+, 141.3 mg L^{-1} SO_4^{2-}, 318.1 mg L^{-1} Cl^-, 0.85 mg L^{-1} NO_3^- and 0.79 mg L^{-1} NO_2^-.

2.3. Pre-pilot plant

A scheme of the 2.5 L pre-pilot plant used to degrade the insecticide is presented in Fig. S1. In each assay, the solution was introduced into the reservoir and recirculated with a centrifugal pump, keeping the flow rate at 200 L h^{-1} with a flowmeter and the temperature at 35 ºC with two heat exchangers. Such temperature was optimal, since it prevented solvent evaporation as well as temperature fluctuations potentially caused by heating upon use of high current and UVA radiation. The electrochemical reactor was an undivided filter-press cell with a 20 cm^2 RuO_2-based plate anode supplied by NMT Electrodes (Pinetown, South Africa) and a 20 cm^2 carbon-PTFE air-diffusion cathode supplied by Sainergy Fuel Cell (Chennai, India), with an interelectrode gap of 1.2 cm. The cathode was fed with atmospheric air at an overpressure of 8.6 kPa regulated with a backpressure gauge and showed a high stability with similar continuous H_2O_2 production during all the trials of this work, as reported previously by us [31-33]. The outlet of this reactor was connected to an annular Schott-Duran glass photoreactor of 10 mm thickness, 110 mm external diameter and 210 mm height (640 mL of irradiated volume). The trials were made at constant *j* controlled by a Grelco GVD310 (0-10 A) power supply, directly providing the cell voltage. Comparative EO-H_2O_2 and EF runs were performed in the dark by covering the system with an opaque cloth, whereas PEF assays were carried out using a 160 W UVA lamp (λ_{max} = 360 nm) from Philips that was centered in the photoreactor. EF and PEF assays were made upon addition of iron(II) sulfate heptahydrate to the solution as catalyst source, before transferring it to the plant reservoir. The salt was completely dissolved Prior to the use of the flow system, the electrodes were cleaned and/or activated under polarization in 0.050 M Na_2SO_4 at *j* = 100 mA cm^{-2} for 240 min. Comparative trials were made with different aqueous matrices including 0.050 M Na_2SO_4, 0.010 M NaCl + 0.043 M Na_2SO_4,

0.035 M NaCl + 0.024 M Na_2SO_4 and 0.070 M NaCl, which presented similar conductivity of 10 mS cm^{-1}.

2.4. Apparatus and analytical procedures

The solution pH was determined with a Crison pH 25 portable pH-meter and the conductivity was measured on a Mehrom 644 conductometer. Samples were collected at regular time intervals and before analysis they were alkalinized to stop the mineralization process and filtered with 0.45 µm PTFE filters purchased from Whatman. The mineralization of carbofuran solutions was assessed from their TOC decay, by injecting 50 µL aliquots into a Shimadzu VCSN TOC analyzer (Kyoto, Japan), yielding reproducible values with ±1% accuracy.

The insecticide concentration abatement was monitored by reversed-phase HPLC employing a Waters 600 LC fitted with a Waters Spherisorb ODS2-C18 5 µm, 150 mm × 4.6 mm (i.d.), column at room temperature and coupled with a Waters 996 photodiode array detector set at λ_{max} = 279.4 nm. Before analysis, the aliquots were diluted with the same volume of methanol in order to stop the degradation process. The mobile phase was acetonitrile/water (10 mM KH_2PO_4, pH 3.0) 1:1 (v/v) eluted at 1 mL min^{-1} and chromatograms displayed a well-defined peak for carbofuran at retention time (t_r) = 5.9 min. Short-chain linear carboxylic acids were detected by ion-exclusion HPLC using the same LC fitted with a Bio-Rad Aminex HPX 87H, 300 mm × 7.8 mm (i.d), column at 35 ºC and the photodiode detector selected at λ = 210 nm. A 4 mM H_2SO_4 solution eluted at 0.6 mL min^{-1} was used as mobile phase. In these chromatograms, peaks appeared at t_r of 7.0 min for oxalic acid, 8.3 min for maleic acid and 14.9 min for fumaric acid.

To identify the primary intermediates generated, several carbofuran solutions in 0.050 M Na_2SO_4 or 0.070 M NaCl at pH 3.0 were electrolyzed for short times by PEF at j = 50 mA cm^{-2}. The organic compounds of each electrolyzed solution were then extracted with 3×25 mL CH_2Cl_2 and the resulting organic solution was dried over Na_2SO_4, filtered and concentrated up to ca. 1 mL to be further analyzed by GC-MS and identified by comparison with NIST05 MS library. GC-MS

was made on an Agilent Technologies system composed of a 7890A GC coupled to a 5975C MS (EI mode at 70 eV). The GC was fitted with a non-polar Agilent J&W HP-5ms 0.25 µm, 30 m × 0.25 mm (i.d.), column. The temperature ramp was: 36 ºC for 1 min, 5 ºC min^{-1} up to 300 ºC and hold time 10 min. The temperature of the inlet, source and transfer line was 250, 230 and 280 ºC.

To assess the toxicity of untreated and treated carbofuran solutions, acute bioluminescence inhibition assays were performed using the marine bacteria *Vibrio fischeri*. This analysis was made by adjusting the pH of all samples to 7, which were subsequently diluted. The acute ecotoxicity of the resulting samples was measured after 15 min of incubation at 25 ºC using an AFNOR T90-301 Microtox® system. The bioluminescent bacteria and other reagents were supplied by Modern Water (New Castle, USA) and the analysis was conducted following the standard procedure recommended by the manufacturer. Results obtained were expressed as EC_{50} (in mg L^{-1}), which accounts for the concentration of solution at a given electrolysis time that causes reduction of the 50% of bioluminescence intensity in 15 min analysis.

3. Results and discussion

3.1. Degradation kinetics of carbofuran in sulfate medium

First, the decay of 0.348 mM carbofuran (corresponding to 50 mg L^{-1} TOC) using the 2.5 L pre-pilot plant was studied in a typical medium of 0.050 M Na_2SO_4 at pH 3.0, j = 100 mA cm^{-2} and 35 ºC for 360 min. The assays were performed under EO-H_2O_2, EF and PEF conditions, with addition of 0.50 mM Fe^{2+} in the two latter processes because this catalyst content was found optimal in analogous treatments of other organics [34-36]. In these runs, the solution pH did not vary substantially, decreasing up to values near 2.6-2.7 due to the formation of acidic byproducts.

Fig. 1a depicts a slow and continuous removal of the insecticide by EO-H_2O_2, achieving a final decrease of 55%. This poor decay of carbofuran for 360 min can be related to its slow oxidation by the low amount of heterogeneous $^{\bullet}OH$ adsorbed onto the active RuO_2-based anode, which is formed

from water oxidation via reaction (1) [33,37,38]. In addition, weaker oxidants like H_2O_2 and its oxidation product $HO_2^{\bullet}$ radical [18,19] exert little influence on the removal of this compound.

$$RuO_2 + H_2O \rightarrow RuO_2(^{\bullet}OH) + H^+ + e^- \quad (1)$$

In contrast, Fig. 1a also shows a remarkable enhancement of the insecticide removal in EF and PEF processes, disappearing after 120 and 90 min of electrolysis, respectively. This reveals that the H_2O_2 produced at the air-diffusion cathode from O_2 gas reduction via reaction (2) originates great quantities of homogeneous $^{\bullet}OH$ in the bulk from Fenton's reaction (3) with added Fe^{2+} [34,39-41]. Fenton's reaction (3) is optimal at pH near 3.0 and can be propagated from Fe^{2+} regeneration from cathodic Fe^{3+} reduction. The superiority of PEF over EF can be accounted for by the additional Fe^{2+} regeneration and $^{\bullet}OH$ production via the photolysis of $Fe(OH)^{2+}$, the pre-eminent Fe(III) species at pH 3.0, according to reaction (4) induced by UVA light in the annular photoreactor [18,40-44].

$$O_{2(g)} + 2H^+ + 2e^- \rightarrow H_2O_2 \quad (2)$$

$$H_2O_2 + Fe^{2+} \rightarrow Fe^{3+} + {}^{\bullet}OH + OH^- \quad (3)$$

$$Fe(OH)^{2+} + hv \rightarrow Fe^{2+} + {}^{\bullet}OH \quad (4)$$

The above concentration decays fit very well to a pseudo-first order kinetics, as presented in Fig. 1b. The corresponding apparent rate constant (k_1) with the R-squared (R^2) thus obtained are summarized in Table 1. The k_1-value in PEF was only 1.65-fold higher than that found in EF, but about 10-fold superior to that obtained in EO-H_2O_2, corroborating the much higher oxidation ability of homogeneous $^{\bullet}OH$ produced from reactions (3) and/or (4) compared to that of $RuO_2(^{\bullet}OH)$ formed from reaction (1). This behavior suggests that the insecticide reacts with a constant amount of $RuO_2(^{\bullet}OH)$ in EO-H_2O_2 and an additional constant amount of $^{\bullet}OH$ in both EF and PEF.

The influence of j on carbofuran decay was also assessed for the powerful PEF treatment. Fig. 2 highlights a gradual upgrading of the insecticide removal rate by increasing j from 25 to 125 mA

cm^{-2}, giving rise to total disappearance in about 120 min at the lowest *j* and in ca. 90 min at the other *j* values. This trend is expected by the progressive enhancement of reaction (1) with higher production of $RuO_2(^{\bullet}OH)$ at a given time as well as of reaction (2), which progressively accelerates the production of H_2O_2 originating larger amounts of $^{\bullet}OH$ in the bulk [19,20]. The inset panel of Fig. 2 shows the good linear trendline obtained for all the concentration decays assuming a pseudo-first order reaction. Nevertheless, the data listed in Table 1 reveal a 1.48-fold increase of the corresponding k_1-value when *j* was increased from 25 to 125 mA cm^{-2}. This is indicative of a loss of relative oxidation ability of the process with raising *j*, which can be explained by a larger extent of parasitic reactions that consume the generated oxidizing species. These reactions include the oxidation of the heterogeneous $^{\bullet}OH$ to O_2 gas from reaction (5), and primordially the dimerization of homogeneous $^{\bullet}OH$ to H_2O_2 from reaction (6) or its destruction by H_2O_2 producing the weaker oxidant hydroperoxyl radical ($HO_2^{\bullet}$) from reaction (7) [19,20]. The gradual drop of the relative oxidation power with increasing *j* is characteristic of EAOPs based on Fenton's reaction chemistry such as EF and PEF, which show similar trends due to the analogous action of the predominant reactions (6) and (7) [39-41].

$$2RuO_2(^{\bullet}OH) \rightarrow 2RuO_2 + O_{2(g)} + 2H^+ + 2e^- \quad (5)$$

$$2^{\bullet}OH \rightarrow H_2O_2 \quad (6)$$

$$H_2O_2 + {}^{\bullet}OH \rightarrow HO_2^{\bullet} + H_2O \quad (7)$$

3.2. Mineralization of carbofuran solutions in sulfate medium

Once assessed the decay kinetics of the insecticide in 0.050 M Na_2SO_4, its long-term mineralization was further investigated. Fig. 3a depicts the TOC removal with electrolysis time for the trials with 0.348 mM carbofuran under the same conditions as those of Fig. 1a. As can be seen, the EO-H_2O_2 process was ineffective for remediation since TOC was only reduced by 4.9% after

360 min of treatment. This means that the chemisorbed $RuO_2(^{\bullet}OH)$ generated from reaction (1), as stated above, cannot convert the byproducts to CO_2. The additional production of large quantities of homogeneous $^{\bullet}OH$ from Fenton's reaction (3) in EF leads to a greater mineralization, reaching 36.1% TOC decay at that time. Note that Fig. 3a shows a continuous TOC abatement until 240 min, whereupon it was strongly decelerated as a result of the formation of byproducts that are more refractory to $RuO_2(^{\bullet}OH)$ and $^{\bullet}OH$. In contrast, a much faster mineralization was observed in PEF, with a final TOC decay of 85.0%, although it was already reduced by 82.4% at 240 min, suggesting again the formation of highly persistent byproducts at long time. This mineralization enhancement can be explained by the additional production of $^{\bullet}OH$ induced from the photolytic reaction (4) upon UVA light irradiation and, to much larger extent, by the photolysis of intermediates like Fe(III) complexes of generated short-chain linear carboxylic acids according to the following general reaction [19,34-36]:

$$Fe(OOCR)^{2+} + h\nu \rightarrow Fe^{2+} + CO_2 + R^{\bullet} \quad (8)$$

The initial N of carbofuran is completely accumulated as ammonium ion upon the action of $^{\bullet}OH$ in other EAOPs [25,29,30]. Consequently, the total mineralization of the insecticide can be written as follows, with a number *n* of electrons of 54:

$$C_{12}H_{15}NO_3 + 21H_2O \rightarrow 12CO_2 + NH_4^+ + 53H^+ + 54e^- \quad (9)$$

and hence, the mineralization current efficiency (MCE) for each trial at a given electrolysis time *t* (in h) and applied current *I* (in A) can be calculated as follows [35,41]:

$$\text{MCE (\%)} = \frac{n\,F\,V\,\Delta(\text{TOC})_{\text{exp}}}{4.32\times10^{7}\,m\,I\,t}\;100 \quad (10)$$

where *F* denotes the Faraday constant (96,485 C mol^{-1}), *V* is the solution volume (in L), $\Delta(TOC)_{exp}$ is the observed TOC decay (in mg L^{-1}), 4.32×10^7 is a conversion factor (= 3600 s h^{-1} × 12000 mg carbon mol^{-1}) and *m* is the number of carbon atoms of carbofuran (12 atoms).

The specific energy consumption per unit TOC mass (EC_{TOC}) for EO-H_2O_2 and EF was obtained from Eq. (11) [35,36]:

$$EC_{TOC}\ (\text{kWh (g TOC)}^{-1}) = \frac{E_{cell}\, I\, t}{V\, \Delta(\text{TOC})_{exp}} \tag{11}$$

where E_{cell} is the average cell voltage (in V), shown on Table 1 for all trials. In the case of PEF, energy consumption was calculated in two modes: (i) from Eq. (11), which disregards the consumption from the UVA lamp because that energy source could be potentially replaced by free sunlight [34,46], and (ii) considering the nominal power of 160 W UVA lamp as follows:

$$EC_{TOC,total}\ (\text{kWh (g TOC)}^{-1}) = \frac{(E_{cell}\, I + 160)\, t}{V\, \Delta(\text{TOC})_{exp}} \tag{12}$$

For subsequent discussion, the values of EC_{TOC} obtained from Eq. (11) have been utilized, since they do not depend on the nominal power of the lamp. However, note that this approach depends on the efficiency of solar photoreactors and the sunlight performance, whose photolytic ability varies with factors including latitude, season and weather.

Fig. 3b and c depicts the change of MCE and EC_{TOC} determined for the assays of Fig. 3a. The data obtained at 240 min of electrolysis are listed in Table 1. All these results agree with the growing oxidation power of EAOPs in the order EO-H_2O_2 << EF < PEF, giving rise to greater TOC removal along with higher MCE and smaller EC_{TOC} values. Thus, Fig. 3b highlights a maximum current efficiency of 27.5% at 90 min of PEF, further undergoing a dramatic decay to 8.9% at 360 min. This drop in MCE can be related to the gradual disappearance of organic matter and the progressive formation of more recalcitrant byproducts [17]. This effect was less substantial in EF and EO-H_2O_2, where very poor MCE values ranging between 3.6% and 5.3% and between 0.5% and 0.8% were obtained, respectively. The EC_{TOC} values for the different treatments decreased in the order EO-H_2O_2 >> EF > PEF, according to their oxidation power (see Table 1). The lowest EC_{TOC} values were attained in PEF, going down to 0.54 kWh (g TOC)$^{-1}$ at 90 min and up to 1.68 kWh (g TOC)$^{-1}$ at the end of the treatment. Considering an industrial price of 0.096 € kWh^{-1} on

average in Spain, the cost of EO-H_2O_2, EF and PEF after 240 min was 2.60, 0.29 and 0.06 € (g TOC)$^{-1}$, respectively. As expected, the EC_{TOC} values were much lower than those obtained when additionally considering the nominal power of the UVA lamp, $EC_{TOC,total}$, as can be seen in Table 1 upon 240 min of electrolysis. However, this total energy consumption is rather unrealistic, since it depends on the lamp power and the energy loses. Despite this, $EC_{TOC,total}$ for PEF was lower than that for EO-H_2O_2 due to its superior oxidation ability. Table 1 also depicts overblown $EC_{TOC,total}$ values compared to EC_{TOC} ones for subsequent PEF treatments.

The change in acute toxicity of the above treated carbofuran solutions was determined from the assessment of the bioluminescence of *Vibrio fischeri*. Fig. 4 illustrates that the initial EC_{50} value of about 16.3 mg L^{-1} of all solutions underwent different variations depending on the applied method. The EO-H_2O_2 process induced a higher toxicity, with a progressive drop of EC_{50} down to 0.2 mg L^{-1} due to the production of more hazardous byproducts. The same tendency can be observed in EF until 180 min, whereupon smaller toxicity was achieved by the gradual destruction of toxic intermediates. Conversely, PEF promoted a very large toxicity reduction, particularly at times > 240 min when TOC was scarcely removed (see Fig. 3a).

3.3. Effect of operation parameters on the PEF treatment of carbofuran in sulfate medium

To check the oxidation power of PEF treatment of carbofuran solutions in 0.050 M Na_2SO_4, the influence of the main operation parameters that control the production of $RuO_2(^{\bullet}OH)$ and homogeneous $^{\bullet}OH$ radicals was explored, aiming at establishing the best mineralization conditions. The effect of *j* between 25 and 125 mA cm^{-2}, Fe^{2+} content between 0.10 and 1.00 mM and insecticide concentration between 0.174 and 1.060 mM on the mineralization performance is shown in Fig. 5-7, respectively. The results obtained at 240 min of electrolysis are collected in Table 1.

Fig. 5a illustrates that the 0.348 mM carbofuran solution with 0.050 M Na_2SO_4 and 0.50 mM Fe^{2+} at pH 3.0 underwent a faster TOC decay by increasing *j* from 25 to 100 mA cm^{-2} until 120 min of electrolysis, whereupon the effect of *j* on TOC abatement was not remarkable (see inset of Fig.

5a and also Table 1). Further upgrading to j = 125 mA cm^{-2} did not improve the mineralization and thus, TOC was finally reduced by 85.0%-89.2% in all these trials. The analogous mineralization achieved at the end of these treatments suggests a pre-eminent role of the photolytic reactions of intermediates upon UVA irradiation. In agreement with this behavior, Fig. 5b and data of Table 1 show a progressive drop in MCE at raising j, as a result of the concomitant acceleration of parasitic reactions (5)-(7) that reduce the oxidation ability of PEF. At the lowest j = 25 mA cm^{-2}, a maximum current efficiency of 77.6% was determined at 120 min, which finally decayed to 37.4%. This j value also provided the smallest EC_{TOC} values of 0.092 kWh (g TOC)$^{-1}$ at 240 min and 0.13 kWh (g TOC)$^{-1}$ at 360 min, as shown in Table 1 and Fig. 5c, respectively.

The Fe^{2+} concentration is another key variable in PEF since it determines the rate of Fenton's reaction (3) for $^{\bullet}OH$ production. An acceleration of this reaction originates a faster destruction of organics with a quicker generation of photoactive products that can be more rapidly photolyzed by UVA light. Fig. 6a shows a poor TOC removal of the 0.348 mM insecticide solution with 0.050 M Na_2SO_4 at pH 3.0 and j = 50 mA cm^{-2} in the presence of 0.10 mM Fe^{2+}, attaining a final TOC decrease of 72.9%, as a result of the reduced number of events between Fe^{2+} and H_2O_2 generating a small amount of $^{\bullet}OH$. The use of 0.25 mM Fe^{2+} accelerated Fenton's reaction (3) and 84% mineralization was reached. Higher mineralization close to 88% was obtained with both, 0.50 and 1.00 mM Fe^{2+}, although the latter led to a slightly faster TOC removal during the first 60 min of electrolysis (see Fig. 6a). From these findings, the best PEF conditions in the pre-pilot plant are reached operating with ≥ 0.50 mM Fe^{2+}. The small influence of Fe^{2+} contents higher than 0.50 mM on mineralization profiles can be explained by the increase in rate of waste reaction (13) with the consequent consumption of $^{\bullet}OH$ [18,19]. Fig. 6b illustrates that maximum MCE values of 47.7% at 90 min with 0.50 mM Fe^{2+} and 52.4% at 60 min with 1.00 mM Fe^{2+} were achieved, further decaying in a similar at times > 120 min, ending in 18.4%. Fig. 6c reveals the same tendency of EC_{TOC} for both Fe^{2+} contents, attaining 0.45 kWh (g TOC)$^{-1}$ at the end of electrolysis.

$$Fe^{2+} + {}^{\bullet}OH \rightarrow Fe^{3+} + OH^{-} \quad (13)$$

The effect of insecticide concentration was tested using 0.050 M Na_2SO_4 with optimum Fe^{2+} content (0.50 mM) at pH 3.0 and j = 50 mA cm^{-2}. Fig. 7a presents a quite similar TOC abatement of 82.8%, 87.8%, 88.5%, 88.0%, 86.3% for growing carbofuran contents of 0.174, 0.348, 0.522, 0.696 and 1.060 mM after 360 min of PEF treatment. The same behavior can be inferred from the data of Table 1 at 240 min of electrolysis. The analogous TOC removal obtained for all the insecticide concentrations confirms the crucial role of UVA radiation in PEF, favoring the photodecomposition of a similar proportion of intermediates and remaining in solution about 12-17% of hardly oxidizable byproducts. This means that a gradually larger amount of TOC is removed with raising carbofuran content, which entails a decay in rate of parasitic reactions (5)-(7) and favors the presence of larger quantities of $RuO_2(^{\bullet}OH)$ and $^{\bullet}OH$ available to react with organics. This fact is clearly deduced from the corresponding MCE and EC_{TOC} values presented in Fig. 7b and c, respectively, as well as in the data of Table 1. The best results were then found at the highest concentration (1.060 mM), with maximum current efficiency of 74.3% at 240 min that decayed to 54.2% along with final EC_{TOC} = 0.16 kWh (g TOC)$^{-1}$.

The above findings allow concluding that best MCE and EC_{TOC} values for carbofuran mineralization in 0.050 M Na_2SO_4 at pH 3.0 by PEF are achieved when operating at low j values and high insecticide concentrations using 0.50 mM Fe^{2+}.

3.4. Degradation kinetics and mineralization of carbofuran in the presence of Cl^- ion

Since the composition of pesticide wastewater usually includes large amounts of both, SO_4^{2-} and Cl^- ions, the study of the carbofuran abatement by PEF was extended to several matrices containing Cl^- ion. An insecticide concentration of 0.348 mM was chosen and 0.010 M NaCl + 0.043 M Na_2SO_4, 0.035 M NaCl + 0.024 M Na_2SO_4 and 0.070 M NaCl were selected as electrolytes because their conductivity was close to 10 mS cm^{-1}, similar to that of 0.050 M Na_2SO_4. These trials were performed at j = 50 mA cm^{-2} after addition of 0.50 mM Fe^{2+} and adjusting each solution to pH

3.0, with H_2SO_4 for the mixture of electrolytes and HCl for the pure NaCl solution. A slight acidification up to pH 2.6-2.7 was always found after 360 min of electrolysis.

Fig. 8 shows a progressive increase in decay rate of the insecticide with raising Cl^- concentration in the electrolyte. In 0.010 M NaCl + 0.043 M Na_2SO_4, total carbofuran removal was attained in 90 min, close to that reached in 0.050 M Na_2SO_4, whereas its disappearance time was reduced to only 25 and approximately 15 min in 0.035 M NaCl + 0.024 M Na_2SO_4 and 0.070 M NaCl, respectively. This behavior can be associated with the large generation of the strong oxidant active chlorine (Cl_2/HClO) from the oxidation of Cl^- at the surface of Pt, BDD and IrO_2- or RuO_2-based anodes from reactions (14) and (15) [45-47]. The attack of active chlorine formed as Cl^- content is raised over carbofuran molecule, in parallel to that of $RuO_2(^{\bullet}OH)$ and $^{\bullet}OH$, explains the evident acceleration of its decay shown in Fig. 8. Worth mentioning, the oxidation of Cl^- occurs in concomitance with formation of large or low amounts of oxoanions (ClO_3^- and ClO_4^-) when using BDD [45,46] and RuO_2-based [47] anodes, respectively.

$$2Cl^- \rightarrow Cl_{2(aq)} + 2e^- \quad (14)$$

$$Cl_{2(aq)} + H_2O \rightarrow HClO + Cl^- + H^+ \quad (15)$$

The inset panel of Fig. 8 illustrates that the insecticide removal agrees with a pseudo-first order decay kinetics for both Cl^-/SO_4^{2-} mixtures, being the corresponding k_1-values given in Table 1. In these cases, a reaction with a constant quantity of all oxidizing species (Cl_2/HClO, $RuO_2(^{\bullet}OH)$ and $^{\bullet}OH$) is expected. In 0.070 M NaCl, however, no good linear fit was obtained, suggesting that the active chlorine, the most powerful oxidant in this medium, did not achieve a steady state, probably due to the short time required to completely destroy the insecticide molecule.

The TOC abatement of 2.5 L of 0.348 mM insecticide in chloride + sulfate mixtures and 0.070 M NaCl at pH 3.0 by PEF using the pre-pilot plant at j = 50 mA cm^{-2} is depicted in Fig. 9a. A progressively slower mineralization can be observed with increasing Cl^- content. TOC was reduced

by 87.8% in 0.050 M Na_2SO_4, whereas it decreased down to 77.1% in 0.010 M NaCl + 0.043 M Na_2SO_4, 63.2% in 0.035 M NaCl + 0.024 M Na_2SO_4, and 59.9% in 0.070 M NaCl. This same tendency can be inferred from the percentage of TOC removal at 240 min of electrolysis given in Table 1. Note that this behavior is contrary to the faster insecticide decay as Cl^- concentration rises, as highlighted in Fig. 8, ascribed to a larger production of active chlorine (Cl_2/HClO) from reactions (14) and (15). It can then be concluded that the formation of recalcitrant and photostable chlorinated byproducts, with increasing concentration at greater amounts of generated active chlorine, explains the inhibition of mineralization depicted in Fig. 9a. The partial destruction of $RuO_2(^{\bullet}OH)$ and $^{\bullet}OH$ in the presence of Cl^-, yielding weaker radicals ($Cl^{\bullet}$, $ClOH^{\bullet-}$, $Cl_2^{\bullet-}$) [48], cannot be discarded either. According to these findings, a concomitant drop in MCE and rise in EC_{TOC} are expected under these conditions, as can be seen in Fig. 9b and c, respectively, and data given in Table 1. For the most inefficient PEF treatment, i.e., in 0.070 M NaCl, for example, the MCE dropped from 51.7% at 20 min (once all the insecticide was removed (see Fig. 8)) to 12.5% at 360 min, due to the gradual production of recalcitrant chlorinated byproducts. In the same way, a final EC_{TOC} = 0.75 kWh (g TOC)$^{-1}$ was obtained in 0.070 M NaCl, a value much higher than 0.44 kWh (g TOC)$^{-1}$ determined in 0.050 M Na_2SO_4 (see Fig. 9c). Consequently, the presence of large amounts of Cl^- in the reaction medium is detrimental for carbofuran mineralization by PEF.

The change in acute toxicity during the PEF treatment of the carbofuran solution in 0.070 M NaCl was determined as well. The initial EC_{50} value of about 16.8 mg L^{-1} only underwent a discrete increase up to 23.4 mg L^{-1} at 360 min (data not shown). This final value was much lower than that found in 0.050 M Na_2SO_4 (see Fig. 4), suggesting the formation of toxic chloroderivatives in NaCl medium (as confirmed below).

3.5. Identification and evolution of intermediates in the absence and presence of Cl^- ion

GC-MS analysis of the treated solutions with 0.348 mM insecticide in 0.050 M Na_2SO_4 or 0.070 M NaCl at pH 3.0 by PEF in the pre-pilot plant at j = 50 mA cm^{-2} allowed the identification

of 5 heteroaromatics or 6 chlorinated compounds, respectively. They were formed upon oxidation with $RuO_2(^{\bullet}OH)$ and $^{\bullet}OH$ in the former medium, and with active chlorine in the latter one. Tables 2 and 3 summarize the characteristics of the intermediates detected in each matrix.

In 0.050 M Na_2SO_4, Table 2 reveals that carbofuran (**1**) is initially demethylated to yield the carbamate **2a**, which loses the side amide group to form the benzofuranol **3a**. Further hydroxylation in C(3) position of **3a** originates the furandiol **4a**. This intermediate can then undergo further oxidation of the incorporated –OH group to give the benzofuranone **5a**, which is subsequently hydroxylated in C(5) position to finally yield the derivative **6a**. On the other hand, when a 0.070 M NaCl was used as electrolyte, 6 chlorinated intermediates were identified. Table 3 highlights that in this medium, **1** is initially chlorinated in C(5) position yielding the chloroderivative **2b**. This compound can then be chlorinated again, in C(6) position, to form the dichloroderivative **3b**, be hydroxylated at the same position with formation of a methoxy group in C(7) position to yield the chlorobenzofuranol **4b**, or lose the side group giving the chlorobenzofuranol **5b**. Further demethylation of **4b** leads to the chlorobenzofurandiol **6b**, whereas chlorination in C(6) position of **5b** produces the dichlorobenzofuranol **7b**, although it could be formed from **3b** transformation as well. The detection of all these intermediates in 0.070 M NaCl corroborates the formation of recalcitrant chloroderivatives byproducts that hamper the carbofuran mineralization in Cl^- matrices by PEF.

The treated solutions with 0.348 mM carbofuran in 0.050 M Na_2SO_4 under the conditions of Fig. 3a were analyzed by ion-exclusion chromatography in order to identify and follow the evolution of generated short-chain linear carboxylic acids. These chromatograms revealed the formation of small amounts of maleic and fumaric acids, arising from the cleavage of cyclic intermediates, along with high quantities of oxalic acid, originated from the oxidation of the above acids and other longer ones. Oxalic acid is a final byproduct since it is directly transformed into CO_2 [19,20]. Note that under the EF and PEF conditions tested, all these carboxylic acids are

primordially present in solution as Fe(III)–carboxylate complexes because Fe^{2+} is largely converted into Fe^{3+} from Fenton's reaction (3) [33-36]. Fig. 10 highlights that oxalic acid was only accumulated up to contents < 1.0 mg L^{-1} in EO-H_2O_2 due to the very low oxidation power of $RuO_2(^{\bullet}OH)$ (see Fig. 3a). In contrast, this acid was largely accumulated up to a steady concentration of about 25.2 mg L^{-1} in EF, corresponding to 6.8 mg L^{-1} TOC that represents a 21.3% of the carbon organic load (31.9 mg L^{-1}) remaining in the solution (see Fig. 3a). This means that Fe(III)-oxalate complexes are highly stable in EF since they are not destroyed by $RuO_2(^{\bullet}OH)$ or $^{\bullet}OH$. Fig. 10 also shows that the use of UVA light in PEF leads to the complete decarboxylation of these complexes according to reaction (8) after 240 min. Note that the final solution treated by PEF still contained 7.5 mg L^{-1} TOC related to other recalcitrant byproducts, a value much lower than remaining TOC in EF. This confirms that the action of UVA light favors the photolytic degradation not only of the final carboxylic acids, but also of other photoactive intermediates, thus explaining the superiority of PEF over EF.

3.6. Mineralization of carbofuran in urban wastewater

A last assay was made by spiking 0.348 mM carbofuran into 2.5 L of an urban wastewater sample that contained 15.0 mg L^{-1} TOC related to natural organic matter (NOM, mainly corresponding to fulvic, tannic and humic acids) and 0.0090 M Cl^- + 0.0015 M SO_4^{2-}. The pH of this wastewater was adjusted to 3.0 with H_2SO_4 and then, 0.034 M Na_2SO_4 and 0.50 mM Fe^{2+} were added to reach a conductivity near 10 mS cm^{-1}, equal to that of previous synthetic matrices. The resulting wastewater was treated by PEF in the pre-pilot plant at j = 50 mA cm^{-2}. Fig. 11 illustrates the TOC abatement with electrolysis time found under these conditions. As can be seen, a fast TOC decay from 65.0 to 40.6 mg L^{-1} (37.5% TOC reduction) occurred during the first 60 min of treatment, whereupon it underwent a gradual deceleration to reach a value of 23.7 mg L^{-1} (63.5% TOC reduction) at 360 min. The partial mineralization achieved with an evident decrease in degradation rate at long time are indicative of the formation of recalcitrant chloroderivatives from

carbofuran upon attack of active chlorine, although this oxidant could also destroy part of the NOM to produce larger amounts of chlorinated byproducts, which are hardly removed via the synergistic action of $RuO_2(^{\bullet}OH)$, $^{\bullet}OH$ and UVA light. The formation of such chloro-organics induces higher toxicity, as commented in subsection 3.4 for trials in NaCl medium, thus confirming our recent findings on the application of EAOPs in urban wastewater [47].

4. Conclusions

It has been shown that, in 0.050 M Na_2SO_4 at pH 3.0, carbofuran is abated more rapidly in the sequence EO-H_2O_2 << EF < PEF using a 2.5 L pre-pilot plant with a RuO_2-based/air-diffusion cell. A pseudo-first order decay kinetics was always obtained. The homogeneous $^{\bullet}OH$ radical formed via Fenton's reaction in EF and additional $^{\bullet}OH$ generated from photolytic reactions in PEF are much more powerful oxidants than $RuO_2(^{\bullet}OH)$ produced in EO-H_2O_2. The same trend was found for mineralization, attaining 82%-88% TOC decrease in PEF using different *j* values and insecticide concentrations at optimum Fe^{2+} content (0.50 mM), thanks to the powerful degradation action of UVA light on photoactive intermediates. The best PEF performance was then achieved at low *j* values and high carbofuran contents, yielding the greatest current efficiencies and smallest energy consumptions. The acute toxicity rapidly diminished once a high mineralization percentage was reached. When Cl^- content was increased in the medium, carbofuran was more rapidly removed in PEF because of its quicker reaction with gradually greater amounts of active chlorine generated. Conversely, lower TOC abatement was attained due to the larger production of recalcitrant chloroderivatives that are hardly mineralized by $RuO_2(^{\bullet}OH)$, $^{\bullet}OH$ in the bulk and UVA light. This behavior was corroborated by GC-MS analysis, revealing the formation of 4 mono and 2 dichloroderivatives in Cl^--containing medium and 5 heteroaromatics in 0.050 M Na_2SO_4. Oxalic acid was the main carboxylic acid and its Fe(III) complexes remained stable in EF, being rapidly and completely photolyzed under UVA irradiation in PEF. PEF treatment of urban wastewater

spiked with carbofuran only yielded a partial mineralization due to the formation of recalcitrant chloroderivatives.

Acknowledgements

The authors acknowledge financial support from project CTQ2016-78616-R (AEI/FEDER, EU) and FONDECYT project 3160753 (CONICYT, Chile).

References

[1] M. Biziuk, A. Przyjazny, J. Czerwinski, M. Wiergowski, Occurrence and determination of pesticides in natural and treated waters, J. Chromatogr. A 754 (1996) 103-123.

[2] N. Borràs, R. Oliver, C. Arias, E. Brillas, Degradation of atrazine by electrochemical advanced oxidation processes using a boron-doped diamond anode, J. Phys. Chem. A 114 (2010) 6613-6621.

[3] D.R.V. Guelfi, F. Gozzi, I. Sirés, E. Brillas, A. Machulek Jr., S.C. de Oliveira, Degradation of the insecticide propoxur by electrochemical advanced oxidation processes using a boron-doped diamond/air-diffusion cell, Environ. Sci. Pollut. Res. 24 (2017) 6083-6095.

[4] D. Pimentel, Green revolution agriculture and chemical hazards, Sci. Total Environ. 188 (1996) 86-98.

[5] S. Chiron, A. Fernandez-Alba, A. Rodriguez, E. Garcia-Calvo, Pesticide chemical oxidation: State-of-the-art, Water Res. 34 (2000) 366-377.

[6] L. Lu, Y. Ma, M. Kumar, J. Lin, Photochemical degradation of carbofuran and elucidation of removal mechanism, Chem. Eng. J. 166 (2011) 150-156.

[7] G.F. Grawe, T.R. Oliveira, E.A. Narciso, S.K. Moccelini, A.J. Terezo, M.A. Soares, M. Castilho, Electrochemical biosensor for carbofuran pesticide based on esterases from *Eupenicillium shearii* FREI-39 endophytic fungus, Biosens. Bioelectron. 63 (2015) 407-413.

[8] S. Khodadoust, M. Hadjmohammadi, Determination of N-methylcarbamate insecticides in water samples using dispersive liquid-liquid microextraction and HPLC with the aid of experimental design and desirability function, Anal. Chim. Acta 699 (2011) 113-119.

[9] N. Koul, R.S. Lokhande, J.K. Dhar, Assessment of physico-chemical, microbiological and pesticide content in potable water in metropolitan city of Delhi, India, J. Appl. Chem. 1 (2012) 512-518.

[10] J. Pereira dos Anjos, J.B. de Andrade, Determination of nineteen pesticides residues (organophosphates, organochlorine, pyrethroids, carbamate, thiocarbamate and strobilurin) in coconut water by SDME/GC-MS, Microchem. J. 112 (2014) 119-126.

[11] L. Feng, G. Yang, L. Zhu, J. Xu, X. Xu, Y. Chen, Distribution and risk assessment of endocrine-disrupting pesticides in drinking water sources from agricultural watershed, Water, Air, Soil Pollut. 227 (2016) 1-10.

[12] V.K. Gupta, I. Ali, Suhas, V.K. Saini, Adsorption of 2,4-D and carbofuran pesticides using fertilizer and steel industry wastes, J. Colloid Interface Sci. 299 (2006) 556-563.]

[13] P. Mineau, S. Porter, C.U. Meteyer, Carbofuran: Toxicity, Diagnosing Poisoning and Rehabilitation of Poisoned Brids, in: N. Richards (ed.), Carbofuran and Wildlife Poisoning: Global Perspectives and Forensic Approaches, Wiley, Hoboken, NJ, USA, 2011. Ch. 2.

[14] W. Mnif, A.I.H. Hassine, A. Bouaziz, A. Bartegi, O. Thomas, B. Roig, Effect of endocrine disruptor pesticides: A review, Int. J. Environ. Res. Public Health 8 (2011) 2265-2303.

[15] M.A. Vishnuganth, N. Remya, M. Kumar, N. Selvaraju, Photocatalytic degradation of carbofuran by TiO_2-coated activated carbon: Model for kinetic, electrical energy per order and economic analysis, J. Environ. Manage. 181 (2016) 201-207.

[16] M. Popovska-Gorevski, M.L. Dubocovich, R.V. Rajnarayanan, Carbamate insecticides target humans melatonin receptors, Chem. Res. Toxicol. 30 (2017) 574-582.

[17] M. Panizza, G. Cerisola, Direct and mediated anodic oxidation of organic pollutants, Chem. Rev. 109 (2009) 6541-6569.

[18] E. Brillas, I. Sirés, M.A. Oturan, Electro-Fenton and related electrochemical technologies based on Fenton's reaction chemistry, Chem. Rev. 109 (2009) 6570-6631.

[19] I. Sirés, E. Brillas, M.A. Oturan, M.A. Rodrigo, M. Panizza, Electrochemical advanced oxidation processes: today and tomorrow. A review, Environ. Sci. Pollut. Res. 21 (2014) 8336-8367.

[20] F.C. Moreira, R.A.R. Boaventura, E. Brillas, V.J.P. Vilar, Electrochemical advanced oxidation processes: A review on their application to synthetic and real wastewaters, Appl. Catal. B: Environ. 202 (2017) 217-261.

[21] T.K. Lau, W. Chu, N. Graham, Degradation of the endocrine disruptor carbofuran by UV, O_3 and O_3/UV, Water Sci. Technol. 55 (2007) 275-280.

[22] Y.-S. Ma, C.-F. Sung, J.-G. Lin, Degradation of carbofuran in aqueous solution by ultrasound and Fenton processes: Effect of system parameters and kinetic study, J. Hazard. Mater. 178 (2010) 320-325.

[23] B. Lopez-Alvarez, P. Villegas-Guzman, G.A. Penuela, R.A. Torres-Palma, Degradation of a toxic mixture of the pesticides carbofuran and iprodione by UV/H_2O_2: Evaluation of parameters and implications of the degradation pathways on the synergistic effects, Water, Air, Soil Pollut. 227 (2016) 1-13.

[24] L.A. Lu, Y.S. Ma, A. Daverey, J.G. Lin, Optimization of photo-Fenton process parameters on carbofuran degradation using central composite design, J. Environ. Sci. Health B 47 (2012) 553-561.

[25] A.K. Abdessalem, N. Bellakhal, N. Oturan, M. Dachraoui, M.A. Oturan, Treatment of a mixture of three pesticides by photo- and electro-Fenton processes, Desalination 250 (2010) 450-455.

[26] R.J. Singh, L. Philip, S. Ramanujam, Rapid removal of carbofuran from aqueous solution by pulsed corona discharge treatment: Kinetic study, oxidative, reductive degradation pathway, and toxicity assay, Ind. Eng. Chem. Res. 55 (2016) 7201-7209.

[27] L. Pu, J. Gao, Y. Hu, H. Liang, W. Xiao, X. Wang, Oxidation degradation of aqueous carbofuran induced by low temperature plasma, Plasma Sci. Technol. 10 (2008) 348-351.

[28] Q. Wang, A.T. Lemley, Oxidative degradation and detoxification of aqueous carbofuran by membrane anodic Fenton treatment, J. Hazard. Mater. 98 (2003) 241-255.

[29] A.K. Abdessalem, M.A. Oturan, N. Oturan, N. Bellakhal, M. Dachraoui, Treatment of an aqueous pesticides mixture solution by direct and indirect electrochemical advanced oxidation processes, Int. J. Environ. Anal. Chem. 90 (2010) 468-477.

[30] A.K. Abdessalem, N. Oturan, N. Bellakhal, M. Dachraoui, M.A. Oturan, Remediation of water contaminated with pesticides by indirect electrochemical oxidation process electro-Fenton, J. Adv. Oxid. Technol. 11 (2008) 276-282.

[31] A. Thiam, E. Brillas, F. Centellas, P.L. Cabot, I. Sirés, Electrochemical reactivity of Ponceau 4R (food additive E124) in different electrolytes and batch cells, Electrochim. Acta 173 (2015) 523-533.

[32] G. Coria, I. Sirés, E. Brillas, J.L. Nava, Influence of the anode material on the degradation of naproxen by Fenton-based electrochemical processes, Chem. Eng. J. 304 (2016) 817-825.

[33] J.R. Steter, E. Brillas, I. Sirés, On the selection of the anode material for the electrochemical removal of methylparaben from different aqueous media, Electrochim. Acta 222 (2016) 1464-1474.

[34] C. Flox, J.A. Garrido, R.M. Rodríguez, P.L. Cabot, F. Centellas, C. Arias, E. Brillas, Mineralization of herbicide mecoprop by photoelectro-Fenton with UVA and solar light, Catal. Today 129 (2007) 29-36.

[35] E.J. Ruiz, A. Hernández-Ramírez, J.M. Peralta-Hernández, C. Arias, E. Brillas, Application of solar photoelectro-Fenton technology to azo dyes mineralization: Effect of current density, Fe^{2+} and dye concentration, Chem. Eng. J. 171 (2011) 385-392.

[36] F. Gozzi, I. Sirés, A. Thiam, S.C. de Oliveira, A. Machulek Jr., E. Brillas, Treatment of single and mixed pesticide formulations by solar photoelectro-Fenton using a flow plant, Chem. Eng. J. 310 (2017) 503-513.

[37] B. Marselli, J. Garcia-Gomez, P.-A. Michaud, M.A. Rodrigo, Ch. Comninellis, Electrogeneration of hydroxyl radicals on boron-doped diamond electrodes, J. Electrochem. Soc. 150 (2003) D79-D83.

[38] B. Borbón, M.T. Oropeza-Guzman, E. Brillas, I. Sirés, Sequential electrochemical treatment of dairy wastewater using aluminium and DSA-type anodes, Environ. Sci. Pollut. Res. 21 (2014) 8573-8584.

[39] I. Sirés, F. Centellas, J.A. Garrido, R.M. Rodríguez, C. Arias, P.-L. Cabot, E. Brillas, Mineralization of clofibric acid by electrochemical advanced oxidation processes using a boron-doped diamond anode and Fe^{2+} and UVA light as catalysts, Appl. Catal. B: Environ. 72 (2007) 373-381.

[40] A. El-Ghenymy, N. Oturan, M.A. Oturan, J.A. Garrido, P.L. Cabot, F. Centellas, R.M. Rodríguez, E. Brillas, Comparative electro-Fenton and UVA photoelectro-Fenton degradation of the antibiotic sulfanilamide using a stirred BDD/air-diffusion tank reactor, Chem. Eng. J. 234 (2013) 115-123.

[41] A. Bedolla-Guzman, I. Sirés, A. Thiam, J.M. Peralta-Hernández, S. Gutiérrez-Granados, E. Brillas, Application of anodic oxidation, electro-Fenton and UVA photoelectro-Fenton to decolorize and mineralize acidic solutions of Reactive Yellow 160 azo dye, Electrochim. Acta 206 (2016) 307-316.

[42] R. Salazar, E. Brillas, I. Sirés, Finding the best Fe^{2+}/Cu^{2+} combination for the solar photoelectro-Fenton treatment of simulated wastewater containing the industrial textile dye Disperse Blue 3, Appl. Catal. B: Environ. 115-116 (2012) 107-116.

[43] A.R.F. Pipi, A.R. De Andrade, E. Brillas, I. Sirés, Total removal of alachlor from water by electrochemical processes, Sep. Purif. Technol. 132 (2014) 674-683.

[44] A. Thiam, I. Sirés, F. Centellas, P.L. Cabot, E. Brillas, Decolorization and mineralization of Allura Red AC azo dye by solar photoelectro-Fenton: Identification of intermediates, Chemosphere 136 (2015) 1-8.

[45] S. Randazzo, O. Scialdone, E. Brillas, I. Sirés, Comparative electrochemical treatments of two chlorinated aliphatic hydrocarbons. Time course of the main reaction by-products, J. Hazard. Mater. 192 (2011) 1555-1564.

[46] A. Thiam, I. Sirés, E. Brillas, Treatment of a mixture of food color additives (E122, E124 and E129) in different water matrices by UVA and solar photoelectro-Fenton, Water Res. 81 (2015) 178-187.

[47] C. Ridruejo, C. Salazar, P. L. Cabot, F. Centellas, E. Brillas, I. Sirés, Electrochemical oxidation of anesthetic tetracaine in aqueous medium. Influence of the anode and matrix composition, Chem. Eng. J. 326 (2017) 811-819.

[48] J. De Laat, G.T. Le, B. Legube, A comparative study of the effects of chloride, sulfate and nitrate ions on the rates of decomposition of H_2O_2 and organic compounds by Fe(II)/H_2O_2 and Fe(III)/H_2O_2, Chemosphere 55 (2004) 715-723.

Figure captions

Fig. 1. (a) Carbofuran concentration decay vs. electrolysis time for the treatment of 2.5 L of 0.348 mM insecticide solutions in 0.050 M Na_2SO_4 at pH 3.0 in the pre-pilot plant of Fig. S1 with a RuO_2-based/air-diffusion cell of 20 cm^2 electrode area at current density (*j*) of 100 mA cm^{-2} and 35 ºC. Method: (○) Electrochemical oxidation with electrogenerated H_2O_2 (EO-H_2O_2), (□) electro-Fenton (EF) with 0.50 mM Fe^{2+} and (◇) photoelectro-Fenton (PEF) with 0.50 mM Fe^{2+} and 160 W UVA lamp. (b) Pseudo-first order kinetic analysis for the above concentration profiles.

Fig. 2. Effect of current density on carbofuran removal vs. time for the PEF treatment of 2.5 L of a 0.348 mM insecticide solution in 0.050 M Na_2SO_4 with 0.50 mM Fe^{2+} at pH 3.0 and 35 ºC using the pre-pilot plant with a RuO_2-based/air-diffusion cell. Current density: (▽) 25 mA cm^{-2}, (○) 50 mA cm^{-2}, (◇) 100 mA cm^{-2} and (△) 125 mA cm^{-2}. The inset panel shows the corresponding kinetic analysis assuming a pseudo-first order reaction for carbofuran.

Fig. 3. (a) TOC removal and variations of (b) mineralization current efficiency and (c) specific energy consumption per unit TOC mass with electrolysis time for the trials of Fig. 1a. Method: (○) EO-H_2O_2, (□) EF with 0.50 mM Fe^{2+} and (◇) PEF with 0.50 mM Fe^{2+} and 160 W UVA lamp.

Fig. 4. Evolution of EC_{50} at 15 min for the treatments of Fig. 3a. Method: (○) EO-H_2O_2, (□) EF with 0.50 mM Fe^{2+} and (◇) PEF with 0.50 mM Fe^{2+} and 160 W UVA lamp.

Fig. 5. Change of (a) TOC, (b) mineralization current efficiency and (c) specific energy consumption per unit TOC mass with electrolysis time for the PEF assays presented in Fig. 2. Current density: (▽) 25 mA cm^{-2}, (○) 50 mA cm^{-2}, (◇) 100 mA cm^{-2} and (△) 125 mA cm^{-2}. The inset in plot (a) is a zoom of the main graph.

Fig. 6. Effect of catalyst concentration ($[Fe^{2+}]_0$) on the time course of (a) TOC, (b) mineralization current efficiency and (c) specific energy consumption per unit TOC mass for the PEF treatment of

2.5 L of 0.348 mM carbofuran solutions in 0.050 M Na_2SO_4 at pH 3.0 using the pre-pilot plant with a RuO_2-based/air-diffusion cell at j = 50 mA cm^{-2} and 35 ºC. $[Fe^{2+}]_0$: (□) 0.10 mM, (◇) 0.25 mM, (○) 0.50 mM and (△) 1.00 mM.

Fig. 7. Influence of insecticide concentration on (a) TOC removal, (b) mineralization current efficiency and (c) specific energy consumption per unit TOC mass with electrolysis time for the PEF treatment of 2.5 L of carbofuran solutions in 0.050 M Na_2SO_4 with 0.50 mM Fe^{2+} at pH 3.0 in the pre-pilot plant with a RuO_2-based/air-diffusion cell at j = 50 mA cm^{-2} and 35 ºC. $[Carbofuran]_0$: (▽) 0.174 mA, (○) 0.348 mM, (□) 0.522 mM, (◇) 0.696 mM and (△) 1.060 mM.

Fig. 8. Influence of chloride content on carbofuran abatement for the degradation of 2.5 L of 0.348 mM insecticide solutions with 0.50 mM Fe^{2+} at pH 3.0 by PEF using the pre-pilot plant with a RuO_2-based/air-diffusion cell at j = 50 mA cm^{-2} and 35 ºC. Electrolyte composition: (△) 0.070 M NaCl, (◇) 0.035 M NaCl + 0.024 M Na_2SO_4, (□) 0.010 M NaCl + 0.043 M Na_2SO_4 and (○) 0.050 M Na_2SO_4. The pseudo-first order kinetic analysis for carbofuran decay is given in the inset panel.

Fig. 9. Variation of (a) TOC, (b) mineralization current efficiency and (c) specific energy consumption per unit TOC mass with electrolysis time for the PEF trials of Fig. 8. Electrolyte composition: (△) 0.070 M NaCl, (◇) 0.035 M NaCl + 0.024 M Na_2SO_4, (□) 0.010 M NaCl + 0.043 M Na_2SO_4 and (○) 0.050 M Na_2SO_4.

Fig. 10. Evolution of oxalic acid detected by ion-exclusion HPLC during the experiments shown in Fig. 3a. Method: (○) EO-H_2O_2, (□) EF with 0.50 mM Fe^{2+} and (◇) PEF with 0.50 mM Fe^{2+} and 160 W UVA lamp.

Fig. 11. TOC abatement vs. electrolysis time for the PEF treatment of 2.5 L of urban wastewater spiked with 0.348 mM carbofuran, with addition of 0.034 M Na_2SO_4 and 0.50 mM Fe^{2+}, at pH 3.0 and 35 ºC using the pre-pilot plant with a RuO_2-based/air-diffusion cell at j = 50 mA cm^{-2}.

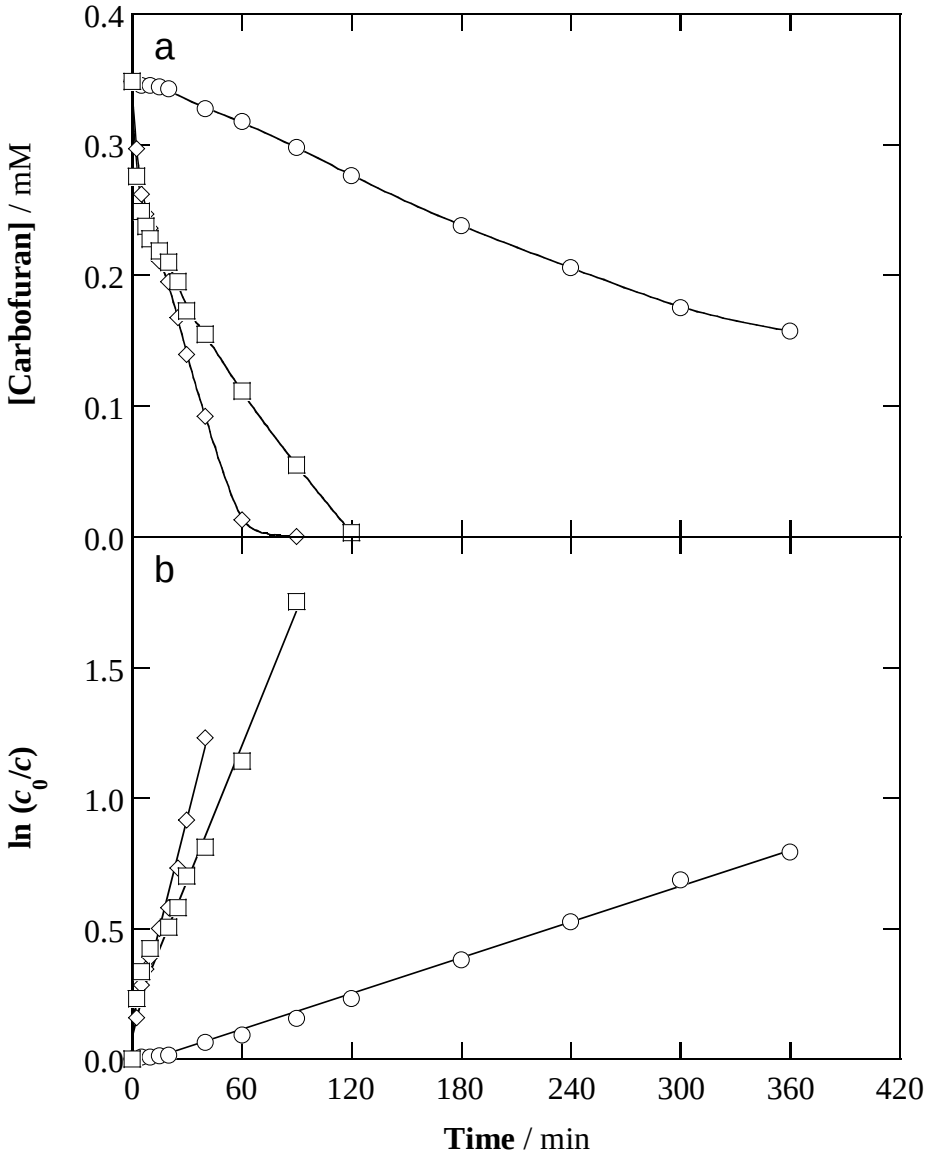
a
b
[Carbofuran] / mM
ln (c_0/c)
Time / min
0.4
0.3
0.2
0.1
0.0
1.5
1.0
0.5
0.0
0
60
120
180
240
300
360
420

Fig. 1

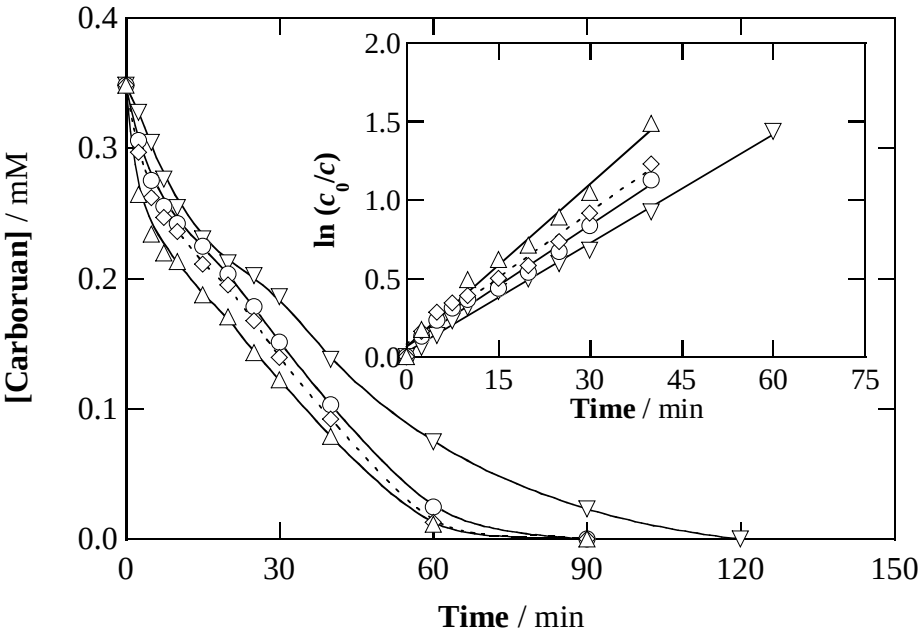
0.4
0.3
0.2
0.1
0.0
[Carboruan] / mM
0
30
60
90
120
150
Time / min
2.0
1.5
1.0
0.5
0.0
ln (c0/c)
0
15
30
45
60
75
Time / min

Fig. 2

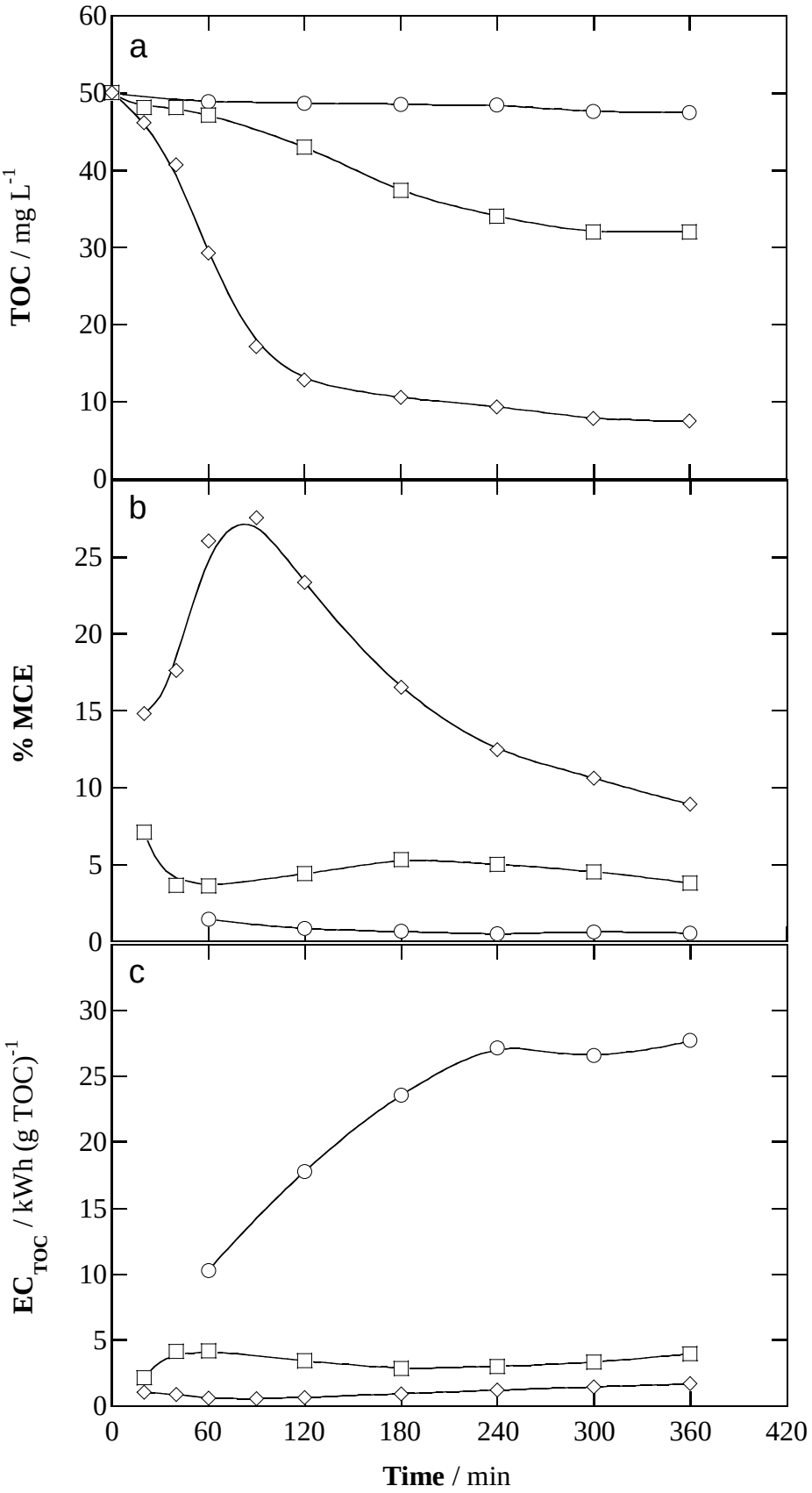
a
b
c
TOC / mg L-1
% MCE
ECTOC / kWh (g TOC)-1
Time / min
0
10
20
30
40
50
60
5
15
25
0
60
120
180
240
300
360
420

Fig. 3

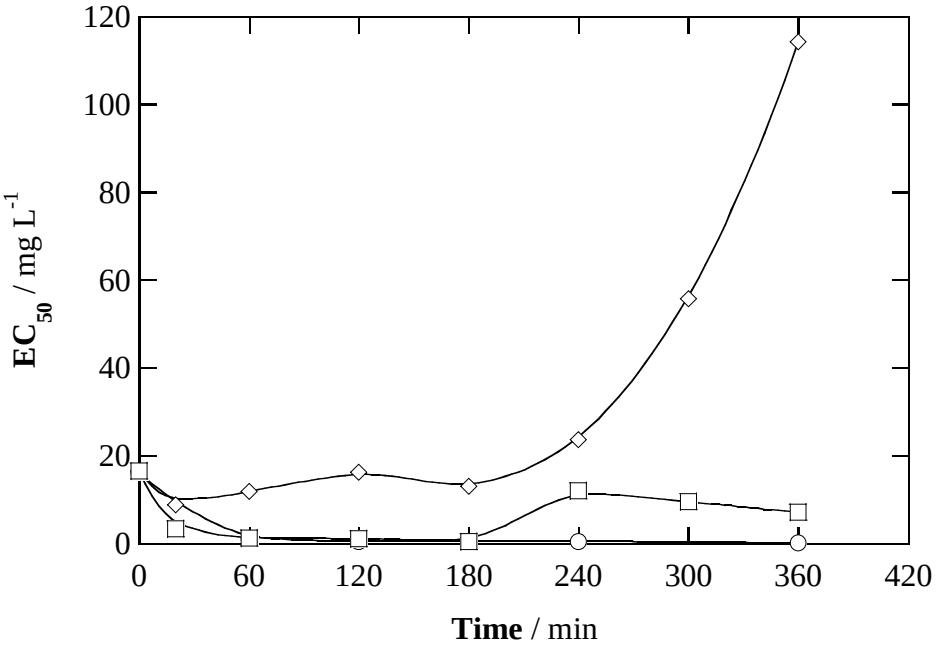
120
100
80
60
40
20
0
0
60
120
180
240
300
360
420
EC50 / mg L-1
Time / min

Fig. 4

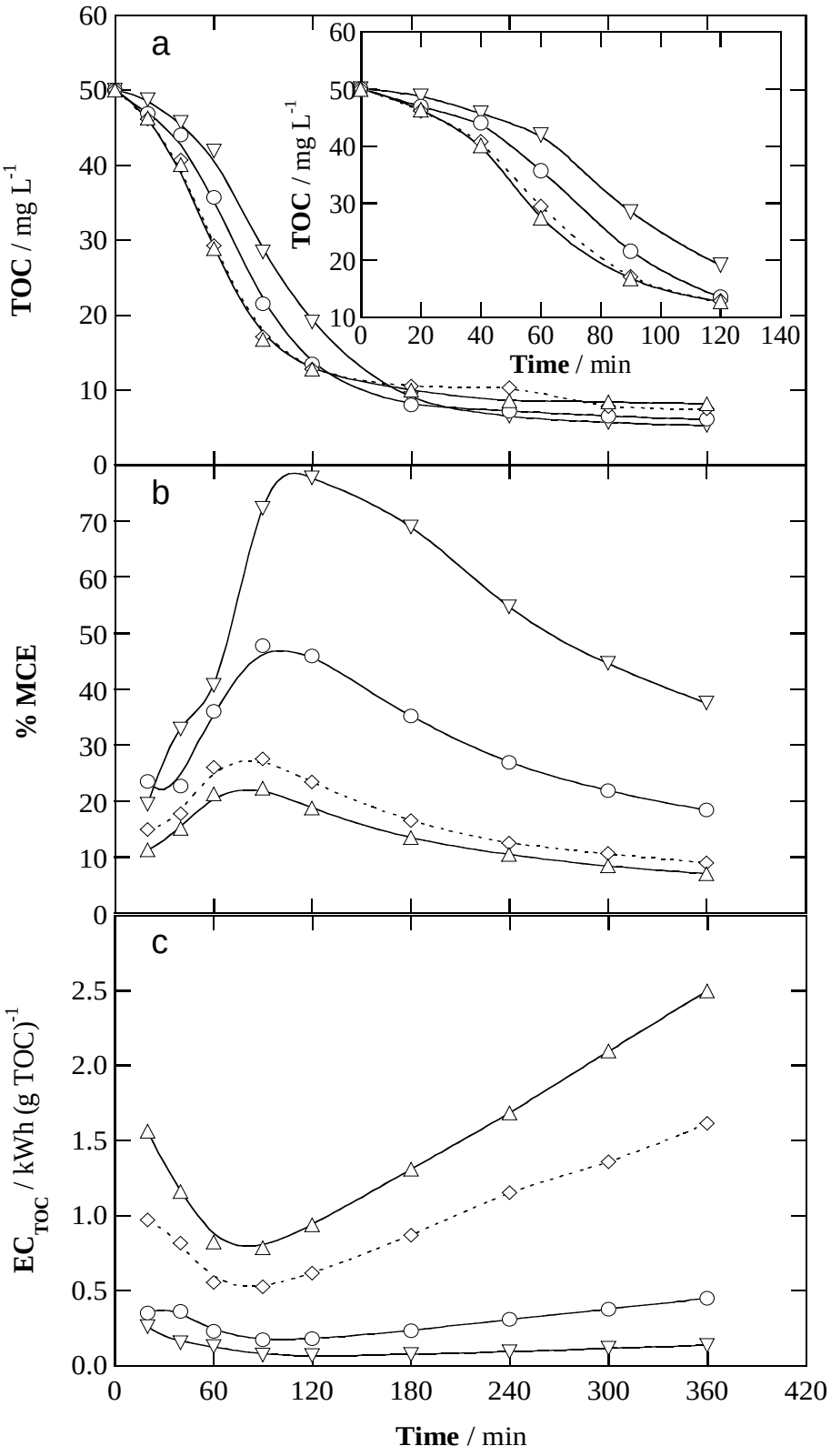

Fig. 5

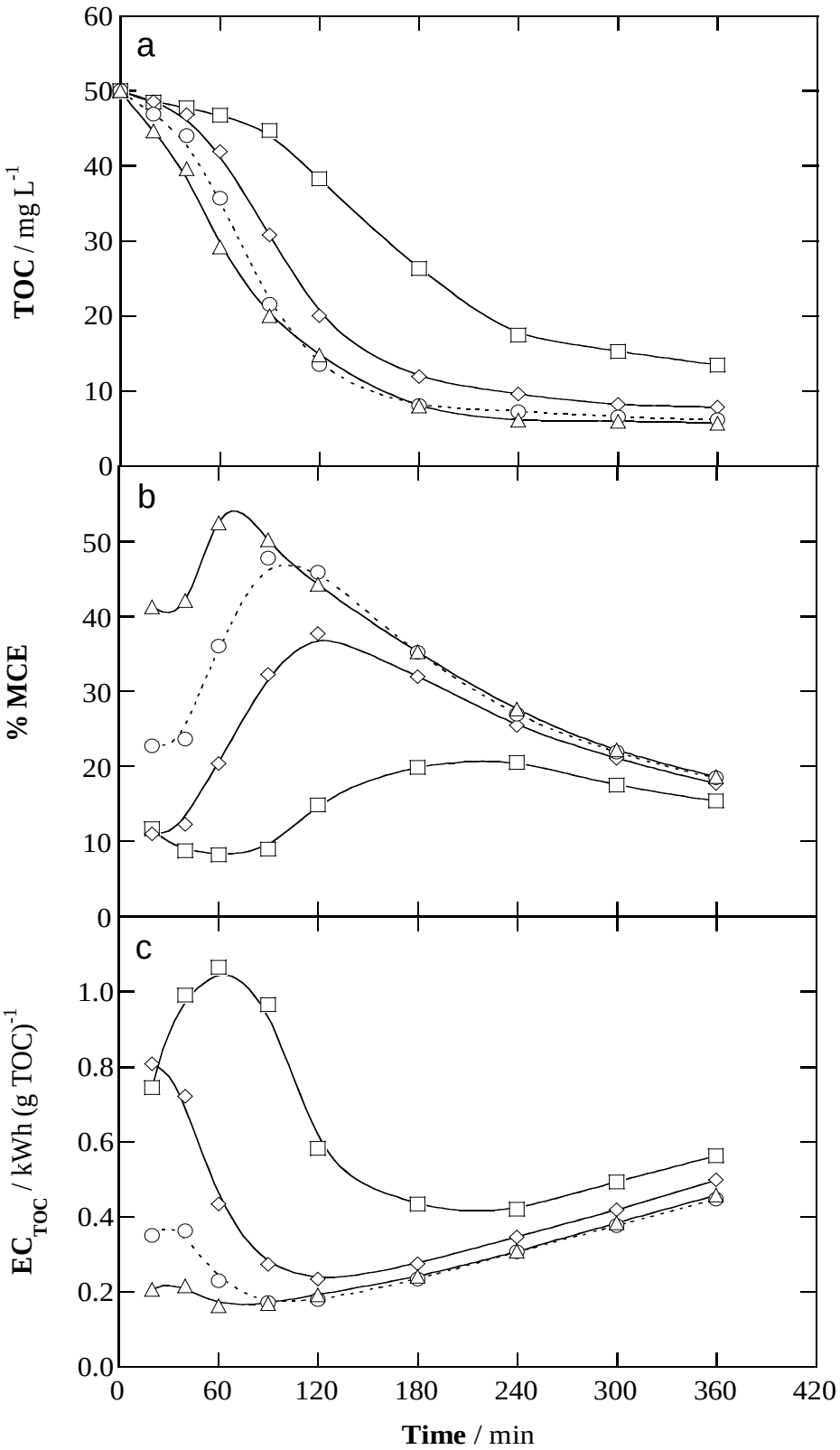
a
b
c
TOC / mg L-1
% MCE
ECTOC / kWh (g TOC)-1
Time / min
0
10
20
30
40
50
60
0.0
0.2
0.4
0.6
0.8
1.0
0
60
120
180
240
300
360
420

Fig. 6

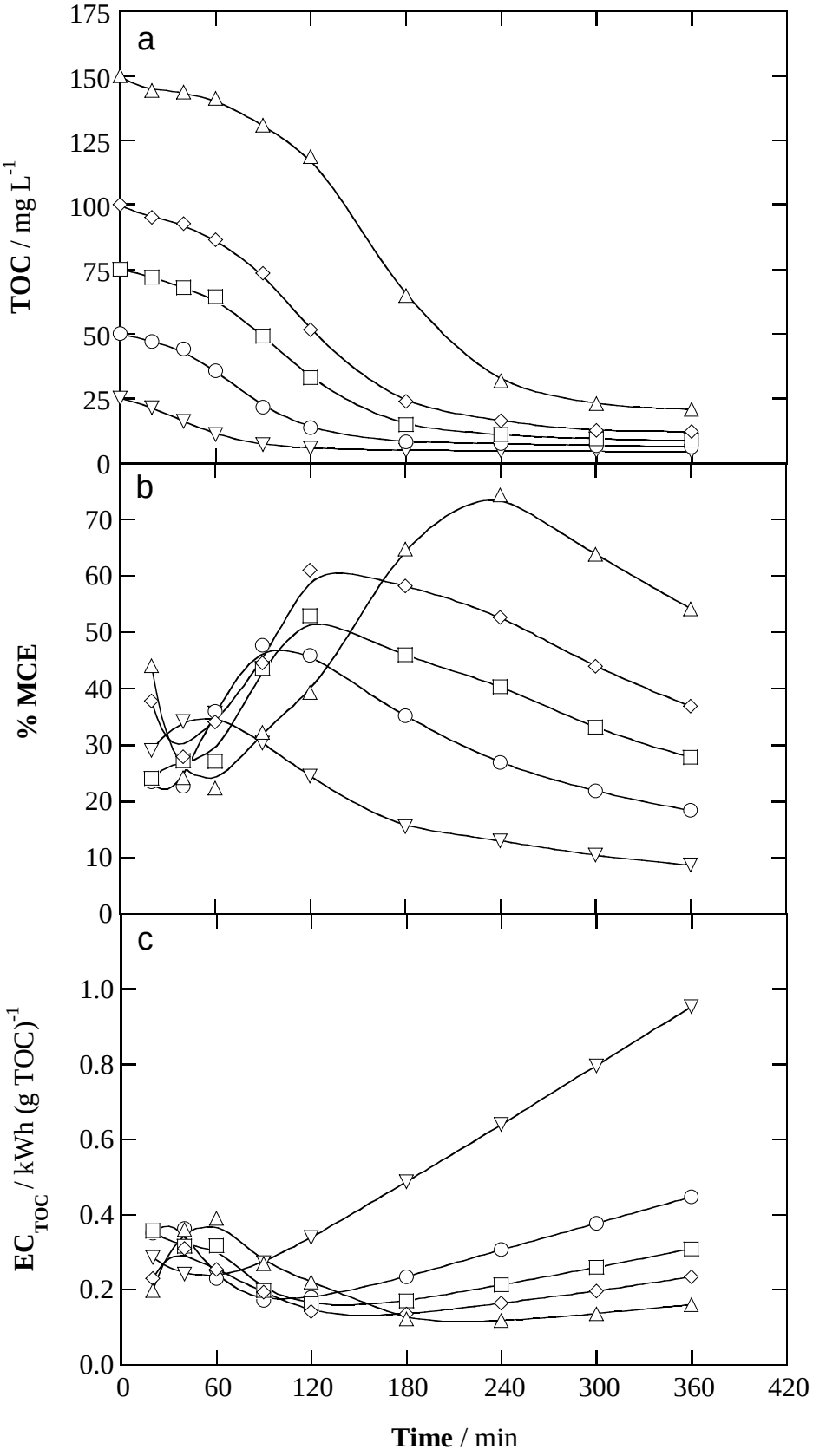
a
b
c
TOC / mg L-1
% MCE
ECTOC / kWh (g TOC)-1
Time / min
0
25
50
75
100
125
150
175
10
20
30
40
60
70
0.0
0.2
0.4
0.6
0.8
1.0
0
60
120
180
240
300
360
420

Fig. 7

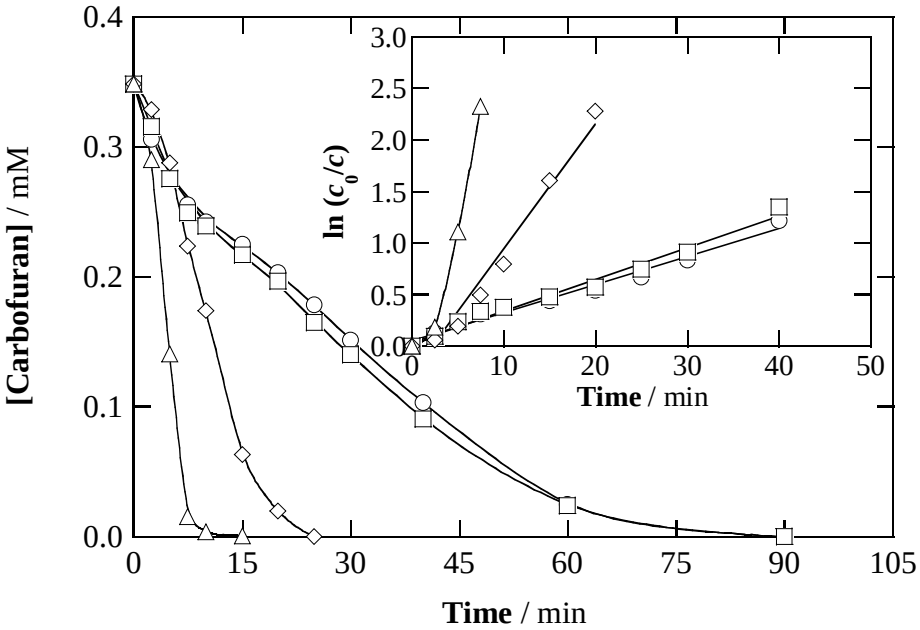
0.4
0.3
0.2
0.1
0.0
[Carbofuran] / mM
0
15
30
45
60
75
90
105
Time / min
3.0
2.5
2.0
1.5
1.0
0.5
0.0
ln (c0/c)
0
10
20
30
40
50
Time / min

Fig. 8

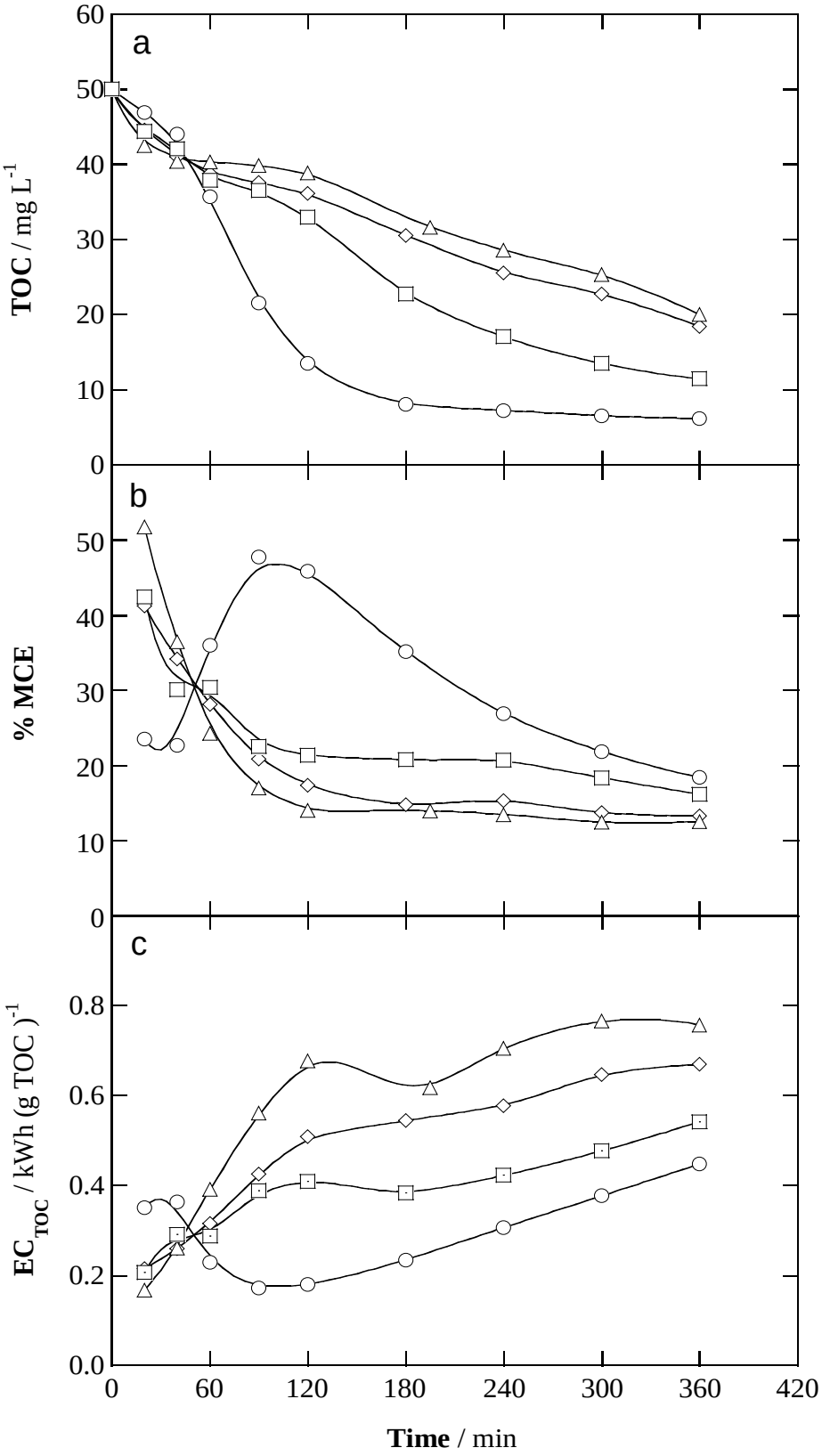
a
b
c
TOC / mg L-1
% MCE
ECTOC / kWh (g TOC)-1
Time / min
0
10
20
30
40
50
60
0.0
0.2
0.4
0.6
0.8
0
60
120
180
240
300
360
420

Fig. 9

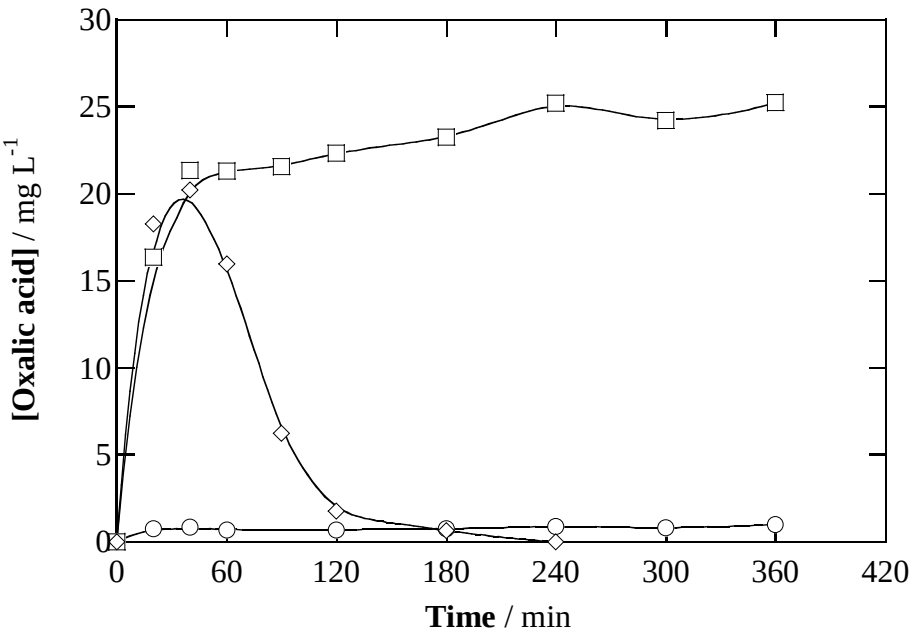
30
25
20
15
10
5
0
0
60
120
180
240
300
360
420
[Oxalic acid] / mg L-1
Time / min

Fig. 10

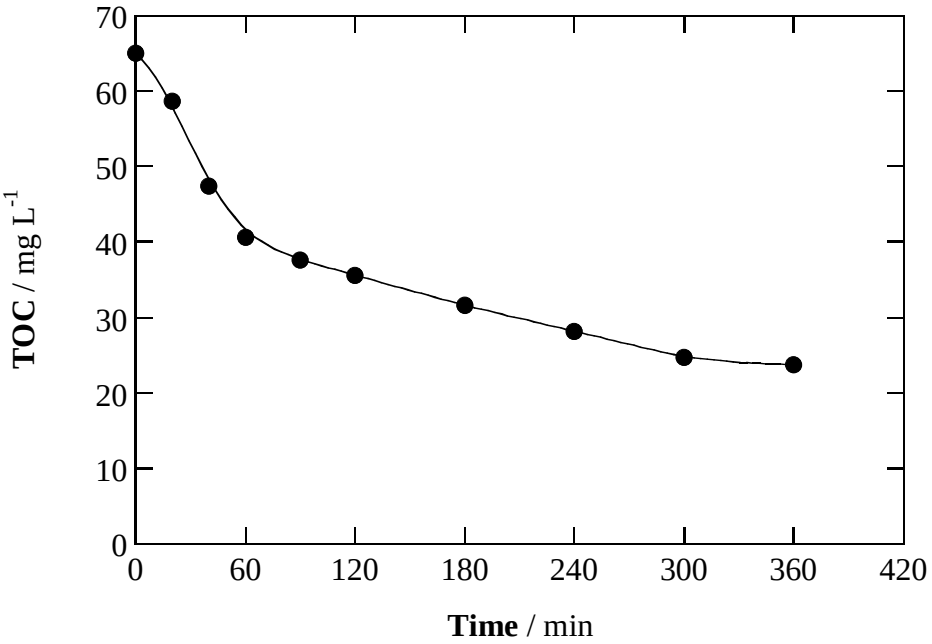
70
60
50
40
30
20
10
0
0
60
120
180
240
300
360
420
TOC / mg L-1
Time / min

Fig. 11

Table 1.

Pseudo-first-order rate constant (k_1) with the corresponding *R*-squared, along with percentage of TOC removal and mineralization current efficiency (MCE), cell voltage and specific energy consumption per unit TOC mass without (EC_{TOC}) and with UV lamp power ($EC_{TOC,total}$) after 240 min of electrolysis of 2.5 L of carbofuran solutions in different media at pH 3.0 and 35.0 ºC upon several EAOPs using the pre-pilot plant with a RuO_2-based/air-diffusion cell.

Method	Electrolyte	$[Carbofuran]_0$ (mM)	$[Fe^{2+}]_0$ (mM)	j (mA cm^{-2})	k_1 (min^{-1})	R^2	% TOC removal	% MCE	E_{cell} (V)	EC_{TOC}[a] (kWh (g TOC)$^{-1}$)	$EC_{TOC,total}$[b] (kWh (g TOC)$^{-1}$)
EO-H_2O_2	0.050 M Na_2SO_4	0.348	-	100	0.003	0.996	3.4	0.5	14.7	27.1	-
EF		0.348	0.50	100	0.017	0.982	32.1	5.0	14.9	2.99	-
PEF		0.174	0.50	50	-[c]	-[c]	81.2	12.9	8.22	0.64	13.2
		0.348	0.50	25	0.023	0.994	89.0	54.6	5.01	0.092	6.9
		0.348	0.10	50	-[c]	-[c]	65.2	20.5	8.56	0.42	8.3
		0.348	0.25	50	-[c]	-[c]	80.8	25.4	8.75	0.35	6.7
		0.348	0.50	50	0.026	0.986	85.6	26.8	8.17	0.30	6.3
		0.348	1.00	50	-[c]	-[c]	88.0	27.6	8.44	0.31	6.1
		0.348	0.50	100	0.028	0.984	82.4	12.4	14.3	1.15	7.4
		0.348	0.50	125	0.034	0.987	82.8	10.4	17.4	1.68	7.9
		0.522	0.50	50	-[c]	-[c]	85.6	40.3	8.53	0.21	4.2
		0.696	0.50	50	-[c]	-[c]	83.8	52.7	8.58	0.16	3.2
		1.060	0.50	50	-[c]	-[c]	79.0	74.3	8.63	0.12	2.3
	0.010 M NaCl + 0.043 M Na_2SO_4	0.348	0.50	50	0.031	0.983	66.0	20.7	8.69	0.42	8.2
	0.035 M NaCl + 0.024 M Na_2SO_4	0.348	0.50	50	0.120	0.975	48.8	15.3	8.79	0.57	11.1
	0.070 M NaCl	0.348	0.50	50	-[d]	-[d]	42.8	13.5	9.43	0.70	12.7

[a] Calculated from Eq. (11)
[b] Calculated from Eq. (12)
[c] Not determined
[d] Fitting according to pseudo-first order kinetics was not good

Table 2.

Primary cyclic products detected by GC-MS during the PEF treatment of 2.5 L of 0.348 mM carbofuran in 0.050 M Na_2SO_4 with 0.50 mM Fe^{2+} at pH 3.0 in the pre-pilot plant with a RuO_2-based/air-diffusion cell at j = 50 mA cm^{-2}.

Number	Compound	Molecular structure	Retention time (min)	Main fragmentation ions (*m*/*z*)
1	2,3-Dihydro-2,2-dimethylbenzofuran-7-yl methylcarbamate (Carbofuran)	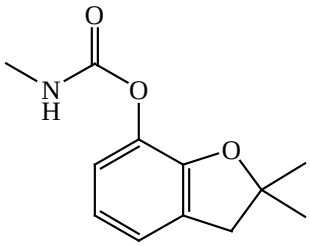	27.95	221, 164, 149
2a	2,3-Dihydro-2,2-dimethylbenzofuran-7-yl carbamate	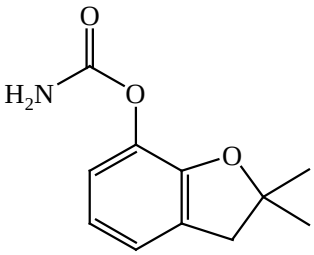	22.62	207, 191
3a	2,3-Dihydro-2,2-dimethyl-7-benzofuranol	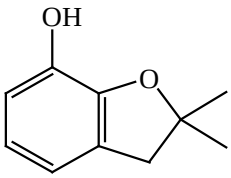	16.48	164, 149, 131
4a	2,3-Dihydro-2,2-dimethyl-3,7-benzofurandiol	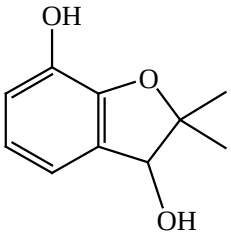	21.36	180, 161, 137
5a	7-Hydroxy-2,2-dimethylbenzofuran-3-one	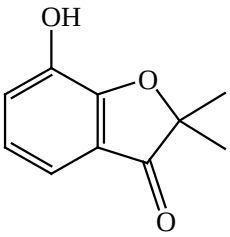	20.32	178, 163, 137
6a	5,7-Dihydroxy-2,2-dimethylbenzofuran-3-one	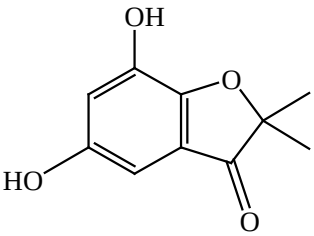	21.78	196, 162, 147

Table 3.

Primary chloroaromatic intermediates identified by GC-MS during the PEF degradation of 2.5 L of 0.348 mM carbofuran in 0.070 M NaCl with 0.50 mM Fe^{2+} at pH 3.0 using the pre-pilot plant with a RuO_2-based/air-diffusion cell at j = 50 mA cm^{-2}.

Number	Compound	Molecular structure	Retention time (min)	Main fragmentation ions (*m*/*z*)
2b	5-Chloro-2,3-dihydro-2,2-dimethylbenzofuran-7-yl methylcarbamate	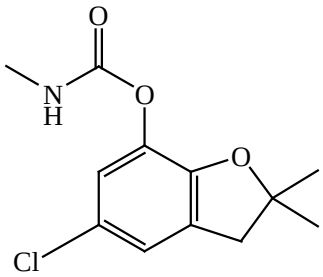	31.31	255
3b	5,6-Dichloro-2,3-dihydro-2,2-dimethylbenzofuran-7-yl methylcarbamate	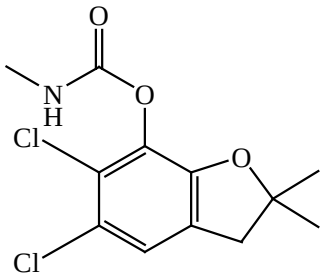	35.92	289
4b	5-Chloro-2,3-dihydro-7-methoxy-2,2-dimethyl-6-benzofuranol	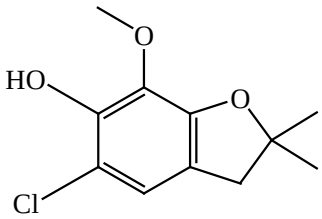	25.67	228, 196, 181
5b	5-Chloro-2,3-dihydro-2,2-dimethyl-7-benzofuranol	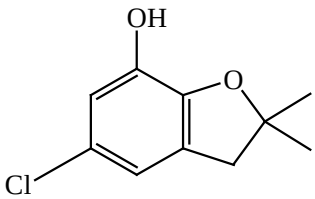	22.96	198, 183, 169
6b	5-Chloro-2,3-dihydro-2,2-dimethyl-6,7-benzofurandiol	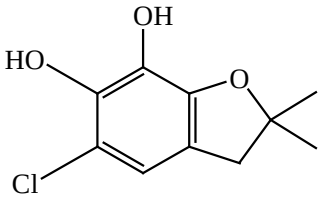	26.75	214
7b	5,6-Dichloro-2,3-dihydro-2,2-dimethyl-7-benzofuranol	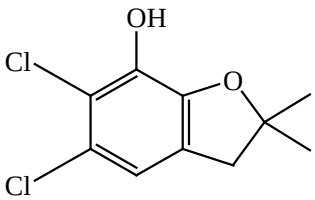	27.64	232, 217, 191